13th International Conference on Aluminum Alloys (ICAA13)
Edited by: Hasso Weiland, Anthony D. Rollett, William A. Cassada
TMS (The Minerals, Metals & Materials Society), 2012

THE EFFECT OF CU AND CR ON CLUSTERING AND PRECIPITATION IN AL-MG-SI ALLOYS

Zeqin Liang[1], Cynthia Sin Ting Chang[2], John Banhart[1,2], Jürgen Hirsch[3]

[1]Helmholtz Zentrum Berlin für Materialien und Energie, Hahn-Meitner-Platz 1, 14109 Berlin, Germany
[2]Technische Universität Berlin, Hardenbergstr. 36/EW 2-3, 10623 Berlin, Germany
[3] Hydro Aluminium Deutschland GmbH, Georg-von-Boeselager-Strasse 21, 53117 Bonn, Germany

Keywords: Al-Mg-Si alloys, thermal analysis, clustering, precipitation

Abstract

A group of alloys based on pure ternary Al-0.4 wt.%Mg-1.0 wt.%Si are used to study the effect of Cu and Cr on clustering and precipitation in Al-Mg-Si alloys. Differential Scanning Calorimetry (DSC) is performed for samples naturally aged for different times after solution heat treatment and ice water quenching. Three clustering processes are observed in all the alloys. The fundamental clustering sequence does not change by additional elements. However, the Cu containing alloy shows less clustering and the first clustering event is hindered. Kissinger analysis reveals that the 2nd and 3rd processes have very similar effective activation energies. Therefore, a model incorporating only two independent reactions is used to obtain kinetic parameters. It is found that the first clustering process starts with a low effective activation energy of 50 kJ/mol and has a mechanism similar to mixed nucleation while the latter two processes are governed by a higher activation energy of 79 kJ/mol and have a mechanism similar to particle growth. During precipitation, the Cr containing alloy shows a similar precipitation heat signal in DSC as the pure ternary, thus having negligible effect on precipitation. On the other hand, the formation of *β"* is less dominant in the Cu-containing alloy while precipitation of other phases before reaching the peak-aged condition is possible.

Introduction

Al-Mg-Si alloys are widely used in automotive industry and architecture due to their potential to be aged to medium strength and their excellent formability and good corrosion resistance. *β"* is considered the main strengthening phases before the alloy reaches its peak aged condition during artificial ageing (AA). The formation of *β"* is influenced by the clustering process during preceding natural ageing (NA), which most of the time implies a negative effect. Clustering is found to take place in different stages that are linked to said negative effect [1, 2]. In order to understand the nature of clustering in Al-Mg-Si alloys, it is necessary to obtain the kinetic parameters which describe the different stages of clustering. On the other hand, when other elements like Cu/Cr exist in the alloy, which is often the case in engineering application, clustering and precipitation behaviour could be influenced. For example, when Cu is added, the precipitation sequence could change. The effect of Cu and Cr on the kinetics of clustering and precipitation is rarely studied and discussed. In this work, three alloys with an amount of Mg and Si similar to a commercial 6016 alloy but with varying amounts of Cu/Cr are used. The stages of clustering are studied and identified by Differential Scanning Calorimetry (DSC). The kinetic parameters of different stages are obtained by fitting with a model combining different processes.

Experimental setup

Three experimental aluminium alloys are being investigated, all provided by Hydro Aluminium Bonn. Their compositions as obtained by OEM are listed in Table I. The alloys have the same nominal Mg and Si content, while two of them also contain a small amount of Cu (0.04%) or Cr (0.02%) typical for commercial alloys. The alloys were received in the cold rolled condition, and all have a thickness of 1 mm. All the DSC measurements were performed in a NETZSCH DSC 204A. The samples were cut and ground to identical discs (scatter in weight: ±2%) and solutionised in an argon atmosphere at 540°C for 1 hour, after which they were ice water quenched. After quenching, DSC measurements were performed with little delay (less than 1 min). Some of the samples underwent natural ageing for 100 min, 1000 min and 10000 min before DSC measurement. Aluminium reference samples with 99.99% purity and similar mass were used to obtain data for the baseline correction for each alloy.

Table I. Composition of the samples investigated in wt.%

alloy	Mg	Si	Cu	Cr	Al
4-10	0.40	1.01	-	-	bal.
4-10Cu	0.37	1.00	0.04	-	bal.
4-10Cr	0.39	1.01	-	0.01	bal.

Results and discussion

Clustering kinetics

Figure 1 shows the clustering peaks of alloy 4-10 without NA, NA for 100 min, 1000 min and 10000 min. Three overlapping clustering peaks are observed in the samples without NA. The 1st and 2nd are located at around 55°C and 85°C, while the 3rd is situated at ~105°C and appears as a shoulder. The 1st peak in the sample NA for 100 min can hardly be observed any more, which shows that after 100 min of NA, the first clustering process has come to an end. In contrast, the 2nd and 3rd peaks are even more significant. The already formed clusters seem to promote the formation of the 2nd and 3rd peaks during the DSC run. As NA proceeds up to 1000 min, the heat signal from the 2nd and 3rd peaks becomes weaker and after 10,000 min of NA only one single peak is observed around 125°C, which corresponds to the 3rd clustering reaction. Moreover the curves decline continuously with increasing temperature, thus indicating that cluster dissolution occurs simultaneously.

Since the clustering peaks overlap with each other, we first consider the entire clustering process and obtain the clustered volume fraction f_i at temperature T_s by

$$f_i = \frac{\int_{T_0}^{T_s} H dT}{\int_{T_0}^{T_e} H dT}, \quad (1)$$

where H is the heat flow measured at a given temperature, $\int_{T_0}^{T_s} H dT$ is then the heat effect from the onset temperature T_0 of clustering reaction to T_s and $\int_{T_0}^{T_e} H dT$ is the heat effect of the total clustering process during the DSC run. The value of f is between 0 and 1, and represents the volume fraction of clusters transformed. The effective activation energy E_{eff} at a fixed volume f is then calculated using Kissinger's method with the following expression [3]:

$$ln\frac{\beta}{T_f^2} = \frac{E_{eff}}{RT_f} + C, \quad (2)$$

where β is the heating rate during the DSC run, T_f the temperature at a fixed *f*, *R* the gas constant and *C* a constant. By plotting ln (β/T_f^2) as a function of *1/T*, the slope of the plot is related to E_{eff}.

Figure 2 shows the changes of E_{eff} with *f* for different samples. For the sample not NA before AA, the initial value of E_{eff} remains fairly stable at ~50 kJ/mol for f≤0.35 after which it increases to ~70 kJ/mol when *f* reaches 0.8. For the sample NA for 100 min before AA, E_{eff} starts to increase from the beginning of the clustering reaction and reaches ~75 kJ/mol when f=0.8, while E_{eff} for 1000 min of NA before AA stays at around 83 to 85 kJ/mol. The low initial E_{eff} value of sample without NA mainly reflects to the first clustering reaction. The stable value indicates that the 2nd and 3rd clustering reactions have not started when f <0.35. Compared to the peaks observed in Figure 1 and the change of E_{eff} in Figure 2, the monotonic increase in the value of E_{eff} observed for the sample NA for 100 min is due to a combined effect of the three clustering reactions. For the sample with 1000 min of NA, where the 2nd clustering reaction is still involved but the change of $E_{eff}$is small, it follows that E_{eff} of the 2nd and 3rd clustering reaction are similar. Therefore the 2nd and 3rd clustering reactions are considered as one single event and the total clustering volume fraction *f* is expressed as [4],

$$f = cf_1 + (1 - c)f_2, \quad (3)$$

where f_1 and f_2 are the volume fractions for the 1st and the 2nd+3rd clustering reactions, respectively. *c* reflects the contribution of the 1st clustering reaction to the changes in the overall transformation.

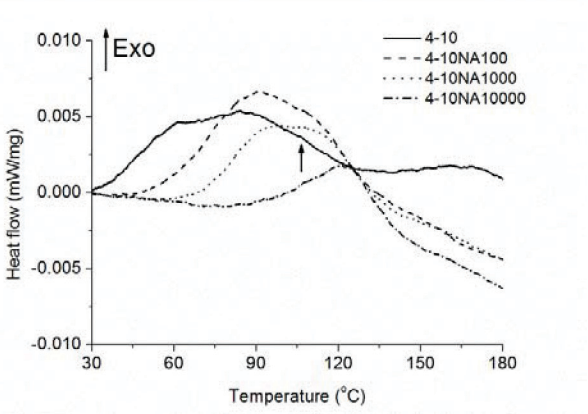

Figure 1. DSC curves of alloy 4-10 after different natural ageing times. The arrow in the graph points at the 3rd clustering reaction appearing as a small shoulder in data of the sample without NA.

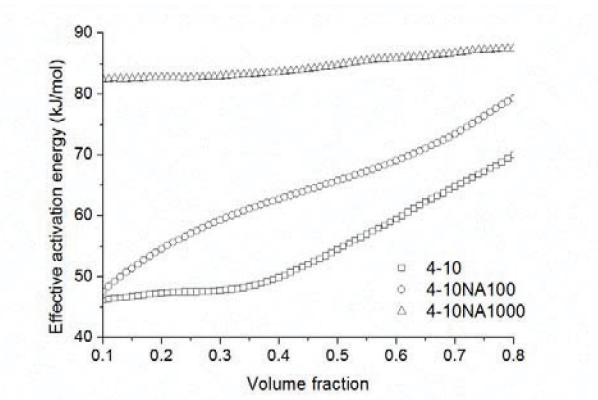

Figure 2. Effective activation energy plotted as a function of volume fraction for the 3 alloys investigated.

Now, for one single process, the fraction transformed can be expressed as:

$$f_i = 1 - (\frac{f_{ext}^i}{\eta_i} + 1)^{-\eta_i}, \quad (4)$$

where η_i is the impingement exponent corresponding to f_1 or f_2 [5]. Assuming that the transformation paths during the DSC run, i.e. with linear heating and for isothermal condition are the same, the extended transformed volume fraction f_{ext}^i can be approximated as [6,7,8]

$$f_{ext}^i \cong (\frac{\beta R}{E_{eff}^i} k_c^i \left[\frac{-E_{eff}^i}{RT}\right] (\frac{T}{\beta})^2)^{n_i}, \quad (5)$$

where n_i is the Avrami exponent.

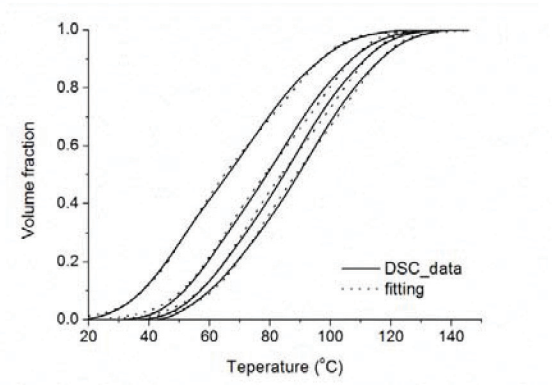

Figure 3. *f* vs. *T* curves with different heating rates for the sample without NA before AA showing the experimental and fitted results (heating rates from left to right: 5 K/min, 10 K/min, 15 K/min and 20 K/min).

The experimental *f* value is fitted, using Eqs. (3) to (5) and the fitted results together with the experimental data for the sample without NA before AA are shown in Fig. 3, the fitted parameters in Table 2. The systemic error of all the results is less than 2%. E_{eff}^1 for samples without NA and 1000 min of NA is 50 kJ/mol, which is similar to the initial E_{eff} obtained by Kissinger's method, see Fig.2. n_1=1.8 indicates that the 1st clustering process resembles a mixture of site saturation and continuous nucleation [9]. Compared to the 1st clustering process, the combined 2nd+3rd clustering process has a higher E_{eff} (79 kJ/mol) and a smaller n value of 1.1. Such a process is similar to particle growth [9]. The value of *c* for sample without NA is

0.67 but then decreases with NA time. For the sample with 1000 min of NA, c=0 and the contribution from the 1st clustering reaction is negligible. Therefore it can be concluded that the 1st clustering process comes to an end before 100 min of NA.

Table 2. Kinetic parameters of clustering from the fitting model.

Alloy	1st clustering			2nd +3rd clustering			c
	E_{eff}^1 (kJ/mol)	k_c^1 ($\times 10^5$ s^{-1})	n_1	E_{eff}^2 (kJ/mol)	k_c^2 ($\times 10^8$s^{-1})	n_2	
4-10	50	7	1.8	79	9.1	1.1	0.67
4-10NA 100	50	7	1.8	79	9.1	1.1	0.08
4-10NA 1000	-	-	-	79	9.1	1.1	0

The effect of Cu and Cr

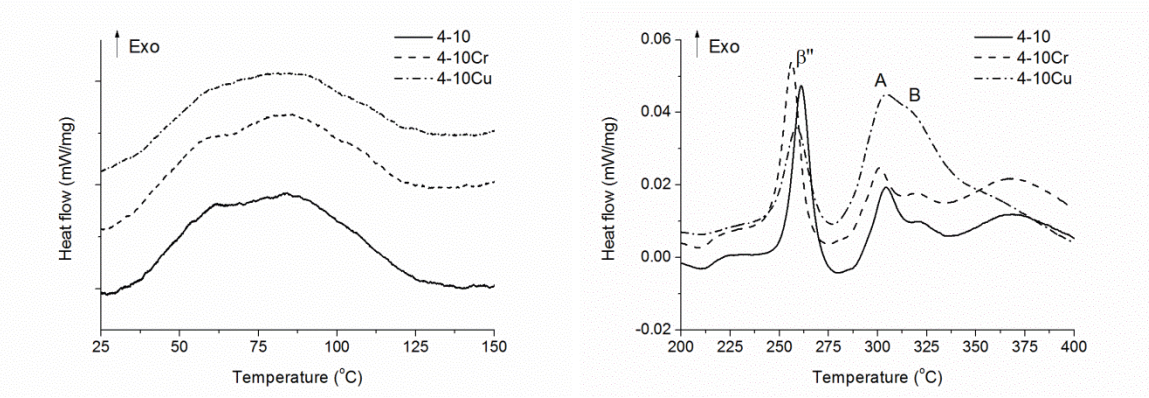

(a) (b)

Figure 4. DSC curves of samples with different compositions. (a) temperature range of clustering , (b) range of precipitation of metastable phases.

The clustering peaks of 4-10, 4-10Cu and 4-10Cr are given in Fig. 4. For clarity, the position of the curves is adjusted by offsets of 0.003 mW/mg and 0.00 6mW/mg for 4-10Cr and 4-10Cu, respectively. Adding Cu or Cr does not affect the clustering kinetics, but the 1st and 2nd overlapping peaks in 4-10Cu become even more difficult to distinguish. The total heat effect found for 4-10Cu is smaller (1.28 J/g) compared to the other alloys (1.54 J/g and 1.43 J/g), showing that the fraction of clusters that can form during NA is less than in the other alloys. The model above is also applied to 4-10Cu and 4-10Cr by fixing E_{eff}, k_c and n according to Table 2 except c. The fitted c in 4-10Cu and 4-10Cr are 0.59 and 0.68 respectively, which indicates that the contribution of the 1st clustering process in 4-10Cu is less significant than in the other alloys.

The DSC signals of precipitation in the temperature range from 200°C to 400°C are shown in Figure 4(b). Three major exothermic reactions are observed in all three alloys. The 1st peak is positioned at around 265°C and corresponds to *β"*[10]. The 2nd (Peak A) and 3rd (Peak B) peaks overlap with each other and are situated between 300°C and 340°C. For the alloy not containing Cu, peak A corresponds to the formation of *β'* [10]. Since the precipitation sequence is different in Cu containing alloys, peak A of 4-10Cu can be associate with *β'*, *Q'* or L formation [11, 12]. Peak B is rarely discussed in the literatures. The precipitation behaviour in 4-10 and 4-10Cr is similar but the peak temperature of *β"* in 4-10Cr is about 5°C lower than in 4-10. 4-10Cu forms less *β"*, but peak A and B are much more pronounced, as revealed in Figure 4(b). This indicates that by adding only 0.04 wt.% Cu, a mixture of different phases can be formed before reaching

the peak aged condition. The kinetic parameters of the formation of *β"* are calculated by a model which incorporates the nucleation growth process. A detailled interpretation and discussion is in preparation and will be published elsewhere [13].

Conclusions

The clustering kinetics of Al-Mg-Si alloys is studied and the effect of Cu and Cr on the clustering and preparation process is discussed:

1. Three stages of clustering are found. A 1st clustering process possesses lower activation energy with a mechanism of mixed nucleation, while the combined 2nd+3rd clustering process has a higher activation energy and resembles particle growth.
2. Cr has a negligible effect on clustering and precipitation in the volume fractions applied.
3. Addition of Cu hinders the 1st clustering process and decreases the total amount of clusters that form. Adding a small amount of Cu influences the precipitation sequence, reduces the dominance of *β"* but increases the fraction of the high temperature phases.

References

1. J. Banhart, C.S.T. Chang, Z. Liang, N. Wanderka, M.D.H. Lay, A.J. Hill, "Natural Ageing in Al-Mg-Si Alloys – A Process of Unexpected Complexity," *Advanced Engineering Materials* 12 (2010) 559-571.
2. J. Banhart, M.D.H. Lay, C.S.T. Chang, A.J. Hill, "The Kinetics of Natural Ageing in Al-Mg-Si Alloys Studied by Positron Annihilation Spectroscopy," *Physical Review B* 83 (2011) 014101.
3. H.E. Kissinger, "Variation of Peak Temperature with Heating Rate in Differential Thermal Analysis," *Journal of Research of the National Bureau of Standards* 57(1956) 217-221.
4. S.V. Vyazovkin, V.I. Goryachko, A.I. Lesnikovich, "An Approach to the Solution of the Inverse Kinetic Problem in the Case of Complex Process. Part III. Parallel Independent Reactions," *Thermochimica Acta* 197(1992) 41-51.
5. M.J. Starink, "On the Meaning of The Impingement Parameter in Kinetic Equations of Diffusion Controlled Reactions," *Journal of Materials Science* 36 (2001) 4433-4441.
6. E. Woldt, "The Relationship between Isothermal and Non-isothermal Description of Johnson-Mehl-Avrami-Kolmogorov Kinetics," *Journal of Physics and Chemistry of Solids* 53 (1992) 521-527.
7. P. Krüger, "On the Relationship between Non-isothermal and Isothermal Kolmogorov-Johnson-Mehl-Avrami Crystallization Kinetics," *Journal of Physics and Chemistry of Solids*, 54 (1993) 1549-1555.
8. M.J. Starink, A.M. Zahra, "An Analysis Method for Nucleation and Growth Controlled Reactions at Constant Heating Rate," *Thermochimica Acta*, 292 (1997) 159-168.
9. J.W. Christian, *The Theory of Transformations in Metals and Alloys* (Killington. UK: Elsevier Science Ltd, 2002), 529-552.
10. K. Matsuda, S. Ikeno, H. Matsui, T. Sato, K. Terayama, Y. Uetani, "Comparison of Precipitates between Excess Si-Type and Balanced-Type Al-Mg_Si alloys during Continuous Heating, " *Metallurgical and Materials Transaction A* 36(2005) 2007-2012.
11. S. Esmaeili, X. Wang, D.J. Lloyd, W.J. Poole, "On the Precipitation-Hardening of Al-Mg-Si-Cu alloy AA6111," *Metallurgical and Materials Transaction A* 34(2003) 751-763.
12. M. Torsæter, W. Lefebvre, C.D. Maioara, S.J. Andersen, J.C. Walmsley, R. Holmestad, "Study of intergrown L and Q' precipitates in Al-Mg-Si-Cu alloys", *Scripta Materialia* 64(2011), 817-820.
13. E. Schmidt, Z. Liang, C.S.T. Chang, J. Banhart, in preparation.